HHS Public Access

Author manuscript

J Gastroenterol Hepatol. Author manuscript; available in PMC 2018 September 01.

Published in final edited form as:

J Gastroenterol Hepatol. 2017 September ; 32(9): 1587–1597. doi:10.1111/jgh.13731.

Prophylactic tributyrin treatment mitigates chronic-binge alcohol-induced intestinal barrier and liver injury

Gail A. Cresci[1,2,3,6], **Bryan Glueck**[1], **Megan R. McMullen**[1], **Wei Xin**[7], **Danielle Allende**[4], and **Laura E. Nagy**[1,5]

[1]Department of Pathobiology, Cleveland Clinic, Cleveland, OH

[2]Department of Gastroenterology/Hepatology, Cleveland Clinic, Cleveland, OH

[3]Pediatric Research Center, Cleveland Clinic, Cleveland, OH

[4]Department of Pathology, Cleveland Clinic, Cleveland, OH

[5]Department of Molecular Medicine, Case Western Reserve University, Cleveland, OH

[6]Department of Medicine, Case Western Reserve University, Cleveland, OH

[7]Department of Pathology, Case Western Reserve University, Cleveland, OH

Abstract

Background/Aim—Impaired gut-liver axis is a potential factor contributing to alcoholic liver disease. Ethanol depletes intestinal integrity and causes gut dysbiosis. Butyrate, a fermentation byproduct of gut microbiota, is altered negatively following chronic ethanol exposure. This study aimed to determine whether prophylactic tributyrin could protect the intestinal barrier and liver in mice during combined chronic-binge ethanol exposure.

Methods—C57BL/6J mice exposed to 5% v/v ethanol-containing diet for 10 days received a single ethanol gavage (5g/kg) 9 hrs prior to euthanasia. Control mice were isocalorically pair-fed maltose dextrin for ethanol. Diets were supplemented (5mM) with tributyrin or glycerol. Intestine and liver disease activity was assessed histologically. Protein and mRNA expression of tight junction proteins (TJ), TLRs and TNFα were assessed. Caco-2 monolayers with/without ethanol exposure and/or sodium butyrate were used to test butyrate's direct effects on intestinal integrity.

Results—Chronic-binge ethanol feeding impaired intestinal TJ protein co-localization staining; however, tributyrin co-treatment mitigated these effects. Ethanol depleted TJ and transepithelial electrical resistance in Caco-2 monolayers, but butyrate co-treatment reduced these effects. Hepatic TLR mRNA expression and TNFα protein expression was induced by ethanol; however, the response was significantly dampened in mice co-treated with tributyrin. Tributyrin altered localization of both neutrophils and single hepatocyte death: leukocytes and apoptotic hepatocytes localized predominantly around the portal tract in ethanol-only treated mice, whereas localization predominated around the central vein in ethanol-tributyrin mice.

Corresponding author: Gail A. Cresci, PhD, RD, Department of Gastroenterology/Hepatology, M17, Cleveland Clinic, 9500 Euclid Avenue, Cleveland, OH 44195, crescig@ccf.org, Phone: 216-445-8317, Fax: 216-444-9415.

Disclosures:
No conflicts of interest, financial or otherwise, are declared by the authors.

Conclusions—Prophylactic tributyrin supplementation mitigated effects of combined chronic-binge ethanol exposure on disruption of intestinal TJ localization and intestinal permeability and liver injury.

Keywords

Tributyrin; gut permeability; chronic-binge ethanol; alcoholic liver disease; tight junction proteins

Introduction

Alcoholic hepatitis (AH) is a syndrome of progressive inflammatory liver injury associated with chronic ethanol intake. An unclear triggering event is responsible for initiation of steatohepatitis in those with hepatic steatosis that continue to consume alcohol [1]. Gut dysbiosis and intestinal permeability are amongst multiple potential implicated triggers[2–6]. Animals and humans exposed to ethanol chronically exhibit overgrowth of opportunistic pathogenic and depletion of beneficial gut bacteria [3–6]. Gut dysbiosis is concerning since the gut-host mutualistic relationship is disrupted potentially jeopardizing benefits this relationship provides including metabolism, host immunity and barrier protection.

Undigested dietary polysaccharides are fermented to yield short-chain fatty acids (SCFA) with acetate, propionate and butyrate predominating in the distal intestine in a nearly constant molar ratio of 60:25:15, respectively[7]. Butyrate, highly important for colonic health, can reach concentrations up to 20 mM in the colon and feces of mammals with normal gut health[7,8]. As butyrate is the primary energy source for colonic mucosal enterocytes[9], molar ratios of butyrate in circulation are comparatively lower than propionate and acetate at physiologic conditions [10]. Butyrate inhibits histone deacetylase and can influence gene expression [11]. Butyrate affects several cellular functions like proliferation and differentiation, increasing normal colonic epithelium proliferation, but decreasing neoplastic colonocyte proliferation *in vitro* and *in vivo* [11–13].

Ethanol causes intestinal barrier impairment and bacterial translocation to the liver; however, underlying mechanisms remain unknown. After being metabolized to acetaldehyde, ethanol is rapidly converted to acetate in the liver and extrahepatic tissues[14]. In humans, 70–80% of oxidized ethanol appears as free acetate in the hepatic vein[15]. Circulating acetate can be transported into the intestinal lumen via monocarboxylate transporters[16]. High-dose ethanol-induced gut dysbiosis is associated with non-physiologic ratios of SCFA in the intestine with elevated luminal acetate levels, but significantly lower butyrate concentrations in the distal intestine [17]. Higher acetate-to-butyrate ratios are associated with increased colonic pathology [18, 19]. Absence of butyrate in intestinal tissue is associated with apoptosis and inflammation [11, 20], and mucosal atrophy, which is reversible in the presence of butyrate [7, 11, 18, 21].

We hypothesized skewed SCFA ratios induced by ethanol exposure contribute to decreased intestinal integrity, increased epithelial cell permeability and promote liver inflammation. This study investigated tributyrin's role in protecting intestinal integrity and consequent liver injury in a combined chronic-binge ethanol mouse model of early stage alcoholic hepatitis.

Materials and Methods

Materials

Glyceryl Tributyrate (tributyrin), sodium butyrate came from Sigma-Aldrich (St. Louis, MO). Pair-fed control diet and Lieber-DeCarli high-fat ethanol diet came from Dyets, Inc (Bethlehem, PA). All primers for quantitative real-time reverse transcription PCR (qRT-PCR) were synthesized by Integrated DNA Technologies (Coralville, IA). Primary antibodies came from the following: anti-occludin (Hycult Biotech, Plymouth Meeting, PA); anti-TNFα (Fitzgerald Industries International, Acton, MA); anti-zonula occluden-1 (Abcam Cambridge, MA); anti-claudin-3 (Invitrogen, Carlsbad, CA).

Methods

Female C57BL/6J mice (8–10 week-old) were purchased from Jackson Laboratories (Bar Harbor, ME). Animals were housed in standard microisolator cages (two animals per cage) and fed standard laboratory chow (rodent diet #2918, Harlan-Teklad, Madison, WI) prior to initiation of liquid diet feeding. All animal procedures were approved by Institutional Animal Care and Use Committee.

Chronic-Binge Ethanol Feeding and Tributyrin Provision

Weight-matched animals were randomly assigned so that each treatment group was within 0.5 gm of each other and then adapted to a control liquid diet for 5 days and allowed either *ad libitum* access to a 5% v/v (27% total kcal) ethanol-containing diet or pair-fed a diet that isocalorically-substituted maltose dextrin for ethanol for 10 days. Diets were made fresh every other day and supplemented with tributyrin (5 mM) or glycerol (5 mM) over the 10 days of ethanol feeding. On Day 11, mice were gavaged with a 5 g/kg dose of ethanol or isocaloric maltose [22]. Included in the gavage at a concentration of 2.5 mM was either tributyrin (7.5 mg) or glycerol (2.3 mg).

Nine hours post gavage, mice were anesthetized and blood was collected from the posterior vena cava by syringe and expelled into EDTA-containing tubes. Livers were weighed and portions fixed in formalin, frozen in Optimal Cutting Temperature (OCT) medium (Sakura Finetek USA, Torrance, CA), snap frozen in liquid nitrogen, or stored in RNAlater (Ambion, Austin, TX) for further analysis. Plasma was separated from whole blood and stored at −80° C. The intestine was dissected and frozen in OCT, snap frozen in liquid nitrogen, or stored in RNAlater.

Histopathology and Immunohistochemistry

Histopathology of the proximal colon—Frozen proximal colon sections were stained with hematoxylin-eosin (HE) for histological observation under an Olympus BX41 light microscope with 100× magnification (10×10). Slides were coded before examination and were evaluated by a single pathologist blinded to treatment. Villus tip-to-crypt depth was measured and mucosal damage was scored as follows [23]: Grade 0: normal structure of intestinal mucosa; Grade 1: subepithelial gap broadened at the apex of the villus, accompanied by capillary blood congestion; Grade 2: subepithelial gap further broadened and epithelial layers separated from the lamina propria; Grade 3: multiple epithelial layers

separated from both sides of villi and a few villi exfoliated; Grade 4: lamina propria exposed because of many exfoliated villi; Grade 5: lamina propria digested and disintegrated, leading to ulceration. Results represent the average of 5–10 crypt lengths per section of tissue. Goblet cells in sections were counted. Ten crypts of intestinal villus in each section were selected and at least three sections per animal were evaluated.

Frozen intestinal sections were used for immunostaining of tight junction (TJ) proteins (claudin-3, occludin, ZO-1). Paraffin embedded liver sections were deparaffinized and stained with hematoxylin and eosin (H&E) or TNFα and then studied by light microscopy. No specific immunostaining was seen in sections incubated with PBS rather than the primary antibody. Slides were coded before examination and a single investigator blinded to treatments viewed them. All images presented represent at least 3 images per tissue section and 4 to 6 mice per experimental condition. Semi-quantification of positive staining was performed using ImagePro plus software (Media Cybernatics, Silver Spring, MD).

Caco-2 Cell Culture—The human colonic epithelial cell line Caco-2 (ATTC, Manassas, VA), a gift from Dr. Christine McDonald, was maintained in Dulbecco's modified Eagle's medium (DMEM; Gibco BRL Products, Grand Island, NY) supplemented with 4.5 g/L glucose, 10% fetal bovine serum (Invitrogen/Gibco), 1% nonessential amino acids and 1% antibiotic solution (penicillin G, streptomycin B; Gibco BRL Products, Grand Island, NY). Cells were grown in 75-cm^2 T-flasks (Fisher, St. Louis, MO) at 37°C/5% CO_2. Medium was changed three times weekly and cells were passaged every 7 to 10 d. Cells were used within 4 passages of each other for this experiment.

Confluent monolayers were harvested by washing the cells with phosphate buffered saline followed by trypsin-EDTA solution. Caco-2 cells were seeded at 1×10^5 density into the apical chamber of a two-chamber cell culture system (Costar Corp., Cambridge, MA) containing a 0.4 cm^2 pore size polycarbonate membrane or into a 24-well plate containing a sterile glass coverslip. Media was changed every 3 days and the cell monolayer allowed to differentiate and polarize over 18–21 days. Cells were pre-treated with sodium butyrate (5 mM) in the apical chamber or on glass coverslips for 18 hours followed by challenge with ethanol (40 mM) for 3 hrs. Caco-2 monolayers seeded on glass coverslips were then rinsed with PBS and fixed with ice-cold methanol followed by immunostaining for TJ proteins.

Measurement of transepithelial electrical resistance—Determination of epithelial barrier function of Caco-2 cell monolayer and integrity of TJs formed between polarized cells was assessed by measurements of transepithelial electrical resistance (TEER) using a EVOM2, Epithelial Volt/Ohm Meter (World Precision Instruments, Sarasota, FL) as previously described (26). Briefly, cells were rinsed with room temperature PBS after which an average of 3 measurements per transwell were recorded. Experiments were performed in triplicate and repeated three times.

Biochemical Assays—Plasma samples from at least 4 to 6 mice per experimental condition were assayed for ALT and AST using commercially available enzymatic assay kits (Sekisui Diagnostics, Lexington, MA) following manufacturer's instructions. Total hepatic

triglycerides were assayed using the Triglyceride Reagent Kit from Pointe Scientific Inc. (Lincoln Park, MI).

qRT-PCR—Total RNA was isolated from liver and proximal colon from at least 4 to 6 mice per experimental condition and 4 mg of total RNA was reverse transcribed as previously described [24]. Real time PCR amplification was performed using PowerSYBR qRT-PCR kits (Applied Biosystems, Grand Island, NY) on an Mx3000p analyzer (Stratagene, La Jolla, CA) for primers: tumor necrosis factor-alpha, zonula occludens-1, occludin, Claudin-1, TLR2, TLR4, TLR9 and 18 S (See Table 1). Relative amount of target mRNA was determined using comparative threshold (Ct) method by normalizing target mRNA Ct values to those of 18S and represented as fold change relative to pair-fed/glycerol mice [24].

Statistical Analysis

Values shown in all figures represent the mean ± SEM (n = 4–8 for pair-fed, n= 6–12 for ethanol-fed; and n=3 experiments for cell culture). Analysis of variance was performed for data with a normal distribution (e.g., Shapiro-Wilk, Pr < W, p >0.05) using the general linear models procedure (SAS, Carey, IN). Data were log-transformed as necessary to obtain a normal distribution. Follow-up comparisons were made by least square means testing. P values of less than 0.05 were considered significant.

Results

Tributyrin supplementation mitigated ethanol-induced disruption of TJ protein expression and integrity

Ethanol exposure for 10 days followed by a single gavage exhibited no obvious damaging effect on colonic mucosa morphology in mice (Fig 1). As expected per normal histology in proximal colon, an abundance of goblet cells was observed in all groups with counts trending upwards in the EtOH-tributyrin group (Fig 1B). Intestinal trefoil factor (ITF) is synthesized and secreted by goblet cells in small and large intestine and is critical in the formation and stabilization of mucus layer [25]. While EtOH treatment depleted ITF mRNA levels in proximal colon, upward trends in expression was noted in ethanol treated mice supplemented with tributyrin (Fig 1C).

Ethanol exposure caused delocalization of TJ in both the proximal colon (claudin-3, occludin and ZO-1) and ileum (ZO-1 and occludin) (Fig 2A and 3A). Tributyrin co-treatment maintained immunoreactive staining intensity of TJ proteins and co-localization of ZO-1 and occludin to similar patterns visualized in pair-fed mice (Fig 2A and 3A). This protective effect of tributyrin on TJ was found at both mRNA and protein levels in proximal colon, but only protein localization was protected in the ileum as there were no differences in ileal mRNA expression between treatment groups (Fig 2 B–D and Fig 3 B–C).

Butyrate attenuated EtOH-induced redistribution of TJ proteins and decreased TEER in Caco-2 cell monolayers

To test butyrate's direct effect on intestinal epithelial cell integrity disrupted by ethanol, we utilized fully differentiated Caco-2 cell monolayers and evaluated alterations in TJ protein

expression and TEER. When cultured without ethanol, TJs were as evidenced by continuous circumferential and co-localized ZO-1 and occludin staining (Fig 4A). In contrast, EtOH-challenged (40 mM, 3 hr) monolayers demonstrated diminished occludin staining and diminished and diffuse fragmentation of ZO-1 staining (Fig 4A). Pretreating monolayers with butyrate (5 mM) for 18 hours before and then during EtOH exposure attenuated this loss in TJ integrity (Fig 4A). Tight junction protein expression was coupled with TEER, as ethanol challenge diminished TEER (Figure 4B) compared with untreated monolayers. Pretreating the apical compartment with butyrate attenuated TEER reduction in cells exposed to EtOH (Fig 4B).

Tributyrin influenced hepatic expression of Toll-like receptors and the inflammatory cytokine TNF-α

In mice only exposed to ethanol, mRNA expression of TLR2, TLR4, TLR9 was induced but mice co-treated with tributyrin were protected exhibiting similar mRNA expression as animals not exposed to ethanol (Fig 5A–C). Similarly, protein expression patterns demonstrated with IHC in liver of inflammatory cytokine TNFα trended as the TLRs. Animals co-treated with tributyrin during EtOH exposure exhibited a dampened response compared to those treated with ethanol alone (Fig 5D, E). Evaluating the individual mice with positive TNFα staining in each group, 83% of the ethanol-glycerol mice, 50% of pair-fed mice, and 33% of ethanol-tributyrin mice had positive TNFα staining ≥0.2.

Tributyrin mitigated liver injury and induced a differential liver injury pattern in ethanol exposed mice

Ethanol exposed mice had elevated plasma ALT levels, as well as neutrophil infiltration, presence of acidophilic bodies indicative of single hepatocyte death, and steatosis assessed histologically (Fig 6). However, while tributyrin co-treatment protected against elevated ALT levels, quantitatively steatosis and neutrophil infiltration was similar between ethanol treated groups (Fig 6). Interestingly, hepatic localization of neutrophilic and acidophilic bodies was impacted by tributyrin; EtOH-only mice exhibited leukocytes and apoptotic hepatocytes predominantly localized to zone 1 (around the portal tract), whereas in localization in ethanol-tributyrin mice predominated in zone 3 (around the central vein).

Discussion

Chronic-binge ethanol exposure to mice causes hepatic injury development characteristic of early stage alcoholic hepatitis [22]. Here we find that in addition to the negative effects on liver, combined chronic-binge ethanol exposure to mice also impacts intestinal homeostasis, impairing intestinal epithelial cell integrity and barrier function. Importantly, the data presented reveal that prophylactic tributyrin supplementation maintains intestinal barrier function and mitigates certain aspects of liver injury induced by chronic-binge ethanol exposure.

While the animal model of chronic-binge ethanol exposure has emerged as a model for early stage acute hepatitis, its effects on intestinal injury are not well defined [22]. The intestinal barrier shields the host from bacterial invasion, or invasion of other microorganisms and

their toxins. There is strong evidence for translocation of pathogenic bacteria and/or its byproducts to the liver as contributors to ethanol-induced liver injury progression and infections[26,27].

Highly dependent upon dietary factors, it's not surprising that chronic ethanol exposure skews gut microbial balance, depletes key metabolites including SCFA, [17] and potentially allows for opportunistic bacterial infection [3–6]. In humans, dietary changes rapidly and markedly alter fecal microbiota composition [28]. While the current study was not aimed to identify alterations in the gut microbiota or its metabolic byproducts following chronic-binge ethanol exposure, interventions were designed under the assumption that chronic (10 day) ethanol feeding (27% total kcal) would induce gut dysbiosis and skew luminal SCFA ratios. The ability for chronic ethanol exposure to induce gut dysbiosis[2–6,17] and shift the luminal distribution of fatty acids [17, 29] has been reported. Further investigations regarding effects of combined chronic-binge ethanol exposure on alterations in gut microbiota and its fermentation byproducts is warranted.

Two important protective features of the intestinal barrier are mucus and TJ protein complexes. While mucus separates intestinal epithelial cells from the luminal environment, TJ seal the paracellular space between epithelial cells. Bacterial penetration of the colonic inner mucus layer by bacteria triggers inflammation. Goblet cells are integral in maintaining inner mucus layer integrity via rapid turnover [30] and ITF, a member of trefoil factor family and a dominant product of differentiated goblet cells, plays a critical functional role in promoting healing after mucosal damage [31]. Butyrate has a key role in colonic epithelial protection and metabolism and has been shown to stimulate goblet cell quantity and colonic mucus secretion in *in vivo* models of colitis [32, 33]. The lack of differential mucosal injury between treatment groups following chronic-binge ethanol exposure suggest beneficial effects of tributyrin on gut-liver protection are not related to goblet cells.

Although pathological damage to colonic mucosa was lacking, we found chronic-binge ethanol exposure depleted the expression of several key components of the intestinal TJ protein complex. The claudin family and occludin are integral transmembrane proteins that directly interact with cytosolic scaffolding proteins, such as zonula occludens, which in turn anchor the TJ complex to the perijunctional actin cytoskeletal rings in cells [34–36]. Occludin depletion in intestinal epithelial cells *in vitro* and *in vivo* leads to a selective or preferential increase in macromolecule flux, suggesting that occludin plays a crucial role in the maintenance of TJ barrier through the large-channel TJ pathway [37]. Interestingly, despite ethanol's harsh effects on TJ protein localization, tributyrin co-treatment alleviated them. Tributyrin, a prodrug of butyrate, is a structured lipid containing 3 butyrate molecules esterified to a glycerol backbone. Tributyrin, digested by gastric and pancreatic amylase and lipase [38] exhibits its main effects distal to the duodenum Butyrate transporter and receptor expression is highest in the ileum and colon making these intestinal regions highly likely to benefit from tributyrin supplementation [39–42]. In our prior work with experimental models which induce gut dysbiosis, tributyrin supplementation protects the intestine [43, 44]. Butyrate induces differentiation in normal intestinal and colon epithelial cells but induces apoptosis in colon cancer cells[10]. Tested in humans as a potential therapy for malignancies and

hemoglobinopathy, tributyrin delivery is able to increase plasma butyrate to biologically active levels with minimal demonstrated toxicity [45].

Caco-2 cell monolayer model allows for evaluation of the direct effects of butyrate on protecting intestinal TJ and permeability integrity, in the absence of potential interactions between ethanol and other cells, such as immune and goblet cells, involved with intestinal epithelium homeostasis. Corroborating what we found *in vivo*, ethanol treatment depleted TJ assembly in Caco-2 cells. Importantly, butyrate co-treatment not only protected against this effect by maintaining TJ protein expression, but also preserved TEER, a functional measurement of TJ integrity. Our *in vitro* data are in line with other studies reporting SCFA, including butyrate, can enhance TEER in Caco-2 monolayers [46, 47].

In this study tributyrin protected intestinal integrity during ethanol exposure which was linked with reduced hepatic TLR induction, inflammation and injury. Ethanol-induced intestinal barrier disruption opens the opportunity for pathogen associated molecular patterns (PAMPS) to translocate to the liver, activate TLRs, and trigger inflammation contributing to hepatocyte damage [48, 49]. Recently, TLR2 and TLR9 deficient mice showed reduced hepatocellular damage induced by chronic-binge ethanol exposure [50]. These data suggest tributyrin preservation of the intestinal barrier during chronic-binge ethanol exposure may reduce hepatic ligands for TLRs and protect against hepatic inflammation.

We don't yet know the mechanism(s) by which tributyrin protects from ethanol-induced injury. Ethanol exposure induces HDAC gene alterations in liver and peripheral blood [51, 52], with increased HDAC gene expression noted in peripheral blood with chronic ethanol exposure [51] and decreased HDAC gene expression following acute ethanol exposure [51, 52]. As a known histone deacetylase inhibitor, tributyrin provision in a rat model of heptaocarinogenesis resulted in lower HDAC activity and increased histone acetylation of the nuclear protein p53 with increased apoptosis and autophagy[53]. Further studies investigating the role of tributyrin and epigenetic regulation in chronic-binge ethanol exposure is warranted.

Interestingly, histologically localization of inflammatory cells and dying hepatocytes varied between groups of ethanol-fed mice. Richly oxygenated periportal zone 1 is less susceptible to hepatic ischemic injury than zone 3 where oxygen supply is least. Butyrate reduces oxidative stress by influencing intracellular antioxidant activity, DNA repair systems or antioxidant enzymes [9]. Butyrate protected against insulin resistance and non-alcoholic fatty liver disease reducing hepatic proinflammatory parameters via suppression of TNFα, TLR and NF-κB activation [54]. Portal butyrate concentrations from endogenous production are reported as high as 64 uM in humans [55]. Therefore, while these data associate intestinal barrier protection by tributyrin with decreased liver injury, they do not exclude that tributyrin may also have a localized hepato-protective effect. Butyrate entry via the portal vein into periportal zone 1 could counteract the pro-oxidant and inflammatory effects of neutrophils noted to be prevalent in this zone in ethanol-only mice. Short-chain fatty acids, acetate, propionate and butyrate, are agonists with very low potency for several G-protein coupled receptors (e.g., GPR43, GPR41, GPR109A). These receptors are expressed on a multitude of tissues and cell types including adipocytes, intestinal epithelial cells, peripheral blood

mononuclear cells and hepatocytes [56]. Activation of these receptors with SCFA induces anti-inflammatory effects [56, 57]. Further investigations determining the role of tributyrin, G-protein coupled receptors and chronic-binge ethanol-induced hepatic inflammation is warranted.

In conclusion, tributyrin supplementation protected both the intestinal barrier and liver from injury induced by combined chronic-binge ethanol exposure. As newer treatment options for patients with AH are needed, these data support the concept that tributyrin could represent a novel preventative therapy for protection against mild alcoholic hepatitis.

Acknowledgments

We thank Manoa Hui for her assistance in preparation of this manuscript. We thank Michael Deblock and Chaitali Ghosh for their assistance with the TEER experiments.

Grants:

This work was supported in part by the National Institute of Health NIAAA grants F32AA021044 (GAC), K99AA023266 (GAC), U01AA02189 (LEN), P50AA024333 (LEN), P20 AA017837 (LEN); the Case Western Reserve University/Cleveland Clinic CTSA (UL1RR024989); and by the National Institute Of Diabetes And Digestive And Kidney Diseases of the National Institutes of Health (P30DK097948). The content is solely the responsibility of the authors and does not necessarily represent the official views of the National Institutes of Health.

References

1. Orman ES, Odena G, Bataller R. Alcoholic liver disease: pathogenesis, management, and novel targets for therapy. J Gastroenterol Hepatol. 2013; 28(Suppl 1):77–84. [PubMed: 23855300]
2. Yan AW, Fouts DE, Brandl J, Stakel P, Torralba M, Schott E, et al. Enteric dysbiosis associated with a mouse model of alcoholic liver disease. Hepatology. 2011; 53:96–105. [PubMed: 21254165]
3. Bull-Otterson L, Feng W, Kirpich I, Wang Y, Quin X, Liu Y, et al. Metagenomic analysis of alcohol induced pathogenic alterations in the intestinal microbiome and the effect of *Lactobacillus rhamnosus GG* treatment. PLOS One. 2013; 8:e53028. [PubMed: 23326376]
4. Ferrier LBF, Debrauwer L, Chabo C, Langella P, Bueno L, Fioramonti J. Impairment of the intestinal barrier by ethanol involves enteric microflora and mast cell activation in rodents. AmJ Pathol. 2006; 168:1148–54. [PubMed: 16565490]
5. Leclercq S, Matamoros S, Cani PD, Neyrinck AM, Jamar F, Starkel P, et al. Intestinal permeability, gut-bacterial dysbiosis, and behavioral markers of alcohol-dependence severity. Proc Natl Acad Sci USA. 2014; 111:E4485–E4493. [PubMed: 25288760]
6. Mutlu E, Keshavarzian A, Engen P, Forsyth CB, Sikaroodi M, Gillevet P. Intestinal dysbiosis: a possible mechanism of alcohol-induced endotoxemia and alcoholic steatohepatitis in rats. Alcohol Clin Exp Res. 2009; 33:1836–1846. [PubMed: 19645728]
7. Velazquez O, Lederer HM, Rombeau JL. Butyrate and the colonocyte. Implications in neoplasia. Dig Dis Sci. 1996; 41:727–39. [PubMed: 8674394]
8. Canani RB, Di Costanzo M, Leone L, Pedata M, Meli R, Calignano A. Potential beneficial effects of butyrate in intestinal and extraintestinal diseases. World J Gastroenterol. 2011; 17:1519–1528. [PubMed: 21472114]
9. Hamer HM, Jonkers D, Venema K, Vanhoutvin S, Troost FJ, Brummer RJ. Review article: the role of butyrate on colonic function. Aliment Pharmacol Ther. 2008; 27:104–119. [PubMed: 17973645]
10. Wachtershauser ASJ. Rationale for the luminal provision of butyrate in intestinal diseases. Eur J Nutr. 2000; 39:164–71. [PubMed: 11079736]
11. Thangaraju M, Cresci G, Anath S, Digby G, Lambert N, Mellinger J, Ganapathy V. GPR109A is a G-protein coupled receptor for the bacterial fermentation product butyrate and functions as a tumor suppressor in colon. Cancer Res. 2009; 69:2826–32. [PubMed: 19276343]

12. Roediger WE. The starved colon – diminished mucosal nutrition, diminished absorption, and colitis. Dis Colon Rectum. 1990; 33:858–62. [PubMed: 2209275]
13. Scheppach WBH, Richter F. Role of short-chain fatty acids in the prevention of colorectal cancer. European J Cancer. 1995; 31A:1077–80. [PubMed: 7576995]
14. Basuroy S, Sheth P, Mansbach CM, Rao RK. Acetaldehyde disrupts tight junctions and adherens junctions in human colonic mucosa: protection by EGF and L-glutamine. Am J Physiol Gastrointest Liver Physiol. 2005; 289:G367–G75. [PubMed: 15718285]
15. Lundquist F, Tugstrup N, Winkler K, Mellemgaard K, Munck-Petersen S. Ethanol metabolism and the production of free acetate in human liver. J Clin Invest. 1962; 41:955–61. [PubMed: 14467395]
16. Shimoyama Y, Kirat D, Akihara Y, Kawasako K, Komine M, Hirayama K, et al. Expressionof monocarboylate transporter 1 (MCT1) in the dog intestine. J Vet Med Sci. 2007; 69:599–604. [PubMed: 17611355]
17. Xie G, Zhong W, Zhen X, Li Q, Qiu Y, Li H, et al. Chronic ethanol consumption alters mammalian gastrointestinal content metabolites. J Proteome Res. 2013; 12:3297–3306. [PubMed: 23763674]
18. Robinson M, Sellin JH, Weinberg D, Vidican DE, Flemal KL, Rademaker AW. Short chain fatty acid rectal irrigation for left-sided ulcerative colitis: a randomized, placebo controlled trial. Gut. 1997; 40:485–91. [PubMed: 9176076]
19. Weaver GAKJ, Miller TL, Wolin MJ. Short chain fatty acid distributions of enema samples from a sigmoidoscopy population: an association of high acetate and low butyrate ratios with adenomatous polyps and colon cancer. Gut. 1988; 29:1539–43. [PubMed: 3209110]
20. Hass RBR, Luciano L, Reale E, Engelhardt W. Lack of butyrate is associated with induction of Bax and subsequent apoptosis in the proximal colon of guinea pig. Gastroenterology. 1997; 112:875–81. [PubMed: 9041249]
21. Breuer RI, Soergel KH, Lashner BA, Christ ML, Hanauer SB, Vanagunas A, et al. Short chain fatty acid rectal irrigation for left-sided ulcerative colitis: a randomized, placebo controlled trial. Gut. 1997; 40:485–91. [PubMed: 9176076]
22. Bertola A, Mathews S, Ki SH, Wang H, Gao B. Mouse model of chronic and binge ethanol feeding (the NIAAA model). Nat Protoc. 2013; 8:627–637. [PubMed: 23449255]
23. Chang RM, Wen LQ, Chang JX, Fu YR, Jiang ZP, Chen S. Repair of damaged intestinal mucosa in a mouse model of sepsis. World J Emerg Med. 2013; 4:223–8. [PubMed: 25215123]
24. McMullen MR, Pritchard MT, Wang Q, Millward CA, Croniger CM, Nagy LE. Early growth response-1 transcription factor is essential for ethanol induced fatty liver injury in mice. Gastroenterology. 2005; 128:2066–2076. [PubMed: 15940638]
25. Podolsky DK, Lynch-Devaney K, Stow JF, Oates P, Murgue B, DeBeaumont M, Sands BE, Mahida YR. Identification of human intestinal trefoil factor. Goblet cell-specific expression of a peptide targeted for apical secretion. J Biol Chem. 1993; 268:6694. [PubMed: 8454642]
26. Keshavarzian A, Farhadi A, Forsyth CB, Rangan J, Jakate S, Shaikh M, Banan A, Fields JZ. Evidence that chronic alcohol exposure promotes intestinal oxidative stress, intestinal hyperpermeability and endotoxemia prior to development of alcoholic steatohepatitis in rats. J Hepatol. 2009; 50:538–547. [PubMed: 19155080]
27. Lambert JC, Zhou Z, Wang L, Song Z, McClain CJ, Kang YJ. Prevention of alterations in intestinal permeability is involved in zinc inhibition of acute ethanol-induced liver damage in mice. J Pharmocol Exp Ther. 2003; 305:880–886.
28. Wu GD, Chen J, Hoffmann C, Bittinger K, Chen YY, Keilbaugh SA, et al. Linking long-term dietary patterns with gut microbial enterotypes. Science. 2011; 334:105–108. [PubMed: 21885731]
29. Chen P, Torralba M, Tan J, Embree M, Zengler K, Starkel P, van Pijkeren JP, et al. Supplementation of Saturated Long-chain Fatty Acids Maintains Intestinal Eubiosis and Reduces Ethanol-induced Liver Injury in Mice. Gastroenterology. 2015; 148:203–214. [PubMed: 25239591]
30. Johansson MEV. Fast renewal of the distal colonic mucus layers by the surface goblet cells as measured by in vivo labeling of mucin glycoproteins. PLoS ONE. 2012; 7:e41009. [PubMed: 22815896]

31. Itoh H, Inoue N, Podolsky DK. Goblet-cell-specific transcription of mouse intestinal trefoil factor gene results from collaboration of complex series of positive and negative regulatory elements. Biochem J. 1999; 341(Pt 2):461–472. [PubMed: 10393106]
32. Pacheco RG, Esposito CC, Muller LC, Castelo-Branco MT, Quintella LP, Chagas VL, et al. Use of butyrate or glutamine in enema solution reduces inflammation and fibrosis in experimental diversion colitis. World J Gastroenterology. 2012; 28:4278–87.
33. Shimotoyodome A, Mequro S, Hase T, Tokimitsu I, Sakata T. Short chain fatty acids but not lactate or succinate stimulate mucus release in the rat colon. Comp Biochem Physiol A Mol Integr Physiol. 2000; 125:525–31. [PubMed: 10840229]
34. Turner JR. Intestinal mucosal barrier function in health and disease. Nat Rev Immunol. 2009; 9:799–809. [PubMed: 19855405]
35. Miyoshi Y, Tanabe S, Suzuki T. Cellular zinc is required for intestinal epithelial barrier maintenance via the regulation of claudin-3 and occludin expression. Am J Physiol Gastrointest Liver Physiol. 2016; 311:G105–G116. [PubMed: 27151944]
36. Shukla PK, Gangwar R, Manda B, Meena AS, Yadav N, Szabo E, et al. Rapid disruption of intestinal epithelial tight junction and barrier dysfunction by ionizing radiation in mouse colon in vivo: protection by *N*-acetyl-L-cysteine. Am J Physiol Gastrointest Liver Physiol. 2016; 310:G705–G715. [PubMed: 26822914]
37. Al-Sadi R, Khatib K, Guo S, Ye D, Youssef M, Ma T. Occludin regulates macromolecule flux across the intestinal epithelial tight junction barrier. Am J Physiol Gastrointest Liver Physiol. 2011; 300:G1054–G1064. [PubMed: 21415414]
38. Conley BA, Egorin MJ, Tait N, Rosen DM, Sausville EA, Dover G, Fram RJ, Van Echo DA. Phase I study of the orally administered butyrate prodrug, tributyrin, in patients with solid tumors. Clin Cancer Res. 1998; 4:629–34. [PubMed: 9533530]
39. Cuff M, Dyer J, Jones M, et al. The human colonic monocarboxylate transporter isoform 1: its potential importance to colonic tissue homeostasis. Gastroenterology. 2005; 128:676–86. [PubMed: 15765403]
40. Rajendran VM, Binder HJ. Characterization and molecular localization of anion transporters in colonic epithelial cells. Ann N Y Acad Sci. 2000; 915:15–29. [PubMed: 11193571]
41. Tamai I, Takanaga H, Maeda H, Sai Y, Ogihara T, Higashida H, et al. Participation of a proton co-transporter, MCT1, in the intestinal transport of monocarboxylic acids. Biochem Biophys Res Commun. 1995; 214:482–9. [PubMed: 7677755]
42. Thangaraju M, Cresci G, Itagaki S, Mellinger J, Browning D, Berger F, et al. Sodium coupled transport of the short chain fatty acid butyrate by SLC5A8 and its relevance to colon cancer. J Gastrointest Surg. 2008; 12:1773–82. [PubMed: 18661192]
43. Cresci G, Nagy LE, Ganapathy V. *Lactobacillus GG* and Tributyrin Supplementation Reduce Antibiotic-Induced Intestinal Injury. JPEN J Parenteral and Enteral Nutr. 2013; 37:763–74.
44. Cresci G, Bush K, Nagy L. Tributyrin supplementation protects mice from acute ethanol-induced gut injury. Alcoholism: Clinical and Experimental Research. Alcohol Clin Exp Res. 2014; 38:1489–1501. [PubMed: 24890666]
45. Edelman MJ, Bauer K, Khanwani S, Tait N, Trepel J, Karp J, Nemieboka N, et al. Clinical and pharmacologic study of tributyrin: an oral butyrate prodrug. Cancer Chemotherapy and Pharmacology. 2003; 51:439–444. [PubMed: 12736763]
46. Mariadason JM, Barkla DH, Gibson PR. Effect of short-chain fatty acids on paracellular permeability in Caco-2 intestinal epithelium model. Am J Physiol. 1997; 272:G705–12. [PubMed: 9142899]
47. Suzuki T, Yoshida S, Hara H. Physiological concentrations of short-chain fatty acids immediate suppress colonic epithelial permeability. Br J Nutr. 2008; 100:297–305. [PubMed: 18346306]
48. Akira S, Hemmi H. Recognition of pathogen-associated molecular patterns. Immunol Lett. 2003; 85:85–95. [PubMed: 12527213]
49. Inokuchi S, Tsukamoto H, Park E, Liu Z, Brenner D, Seki E. Toll-like receptor 4 mediates alcohol-induced steatohepatitis through bone marrow-derived and endogenous liver cells in mice. Alcohol Clin Exp Res. 2011; 35:1509–1518. [PubMed: 21463341]

50. Roh YS, Zhang B, Loomba R, Seki E. TLR2 and TLR9 contribute to alcohol-mediated liver injury through induction of CXCL1 and neutrophil infiltration. Am J Physiol Gastrointest Liver Physiol. 2015; 309:G30–G41. [PubMed: 25930080]

51. Lopez-Moreno JA, Marcos M, Calleja-Conde J, Echeverry-Alzate V, Buhler KM, Costa-Alba P, et al. Histone Deacetylase Gene Expression Following Binge Alcohol Consumption in Rats and Humans. Alcoholism: Clinical and Experimental Research. 2015; 39:1939–1950.

52. Kirpich I, Ghare S, Zhang J, Gobejishvili L, Kharebava G, Barve SJ, Barker D, Moghe A, McClain CJ, Barve S. Binge alcohol-induced microvesicular liver steatosis and injury are associated with down-regula-tion of hepatic Hdac 1, 7, 9, 10, 11 and up-regulation of Hdac 3. Alcohol Clin Exp Res. 2012; 36:1578–1586. [PubMed: 22375794]

53. De Conti A, Tryndyak V, Kotrubash I, Heidor R, Kuroiwa-Trzmielina J, Ong TP, Beland FA, et al. The chemopreventative activity of the butyric acid prodrug tributyrin in experimental rat hepatocincinogenesis is associated with p53 acetylation and activation of the p53 apoptotic signaling pathway. Carcinogenesis. 2013; 34:1900–6. [PubMed: 23568954]

54. Simeoli R, Russo R, Lacono A, Santoro A, Paciello O, Ferrante MC, Canani RB, Calignano A, Meli R. Effects of sodium butyrate and its synthetic amide derivative on liver Inflammation and glucose tolerance in an animal model of steatosis induced by high fat diet. PlosOne. 2013; 8:e68626.

55. Dankert J, Zijlstra JB, Wolthers BG. Volatile fatty acids in human peripheral and portal blood: quantitative determination vacuum distillation and gas chromatography. Clin Chim Acta. 1981; 110:301–7. [PubMed: 7226534]

56. Ang Z, Ding JL. GPR41 and GPR43 in Obesity and inflammation – Protective or Causative? Frontiers Immunology. 2016; 7 Article 28.

57. Singh N, Guray A, Sivaprakasam S, Brady E, Padia R, Shi H, et al. Activation of Gpr109a, receptor for niacin and the commensal metabolite butyrate, suppresses colonic inflammation and carcinogenesis. Immunity. 2014; 40:128–39. [PubMed: 24412617]

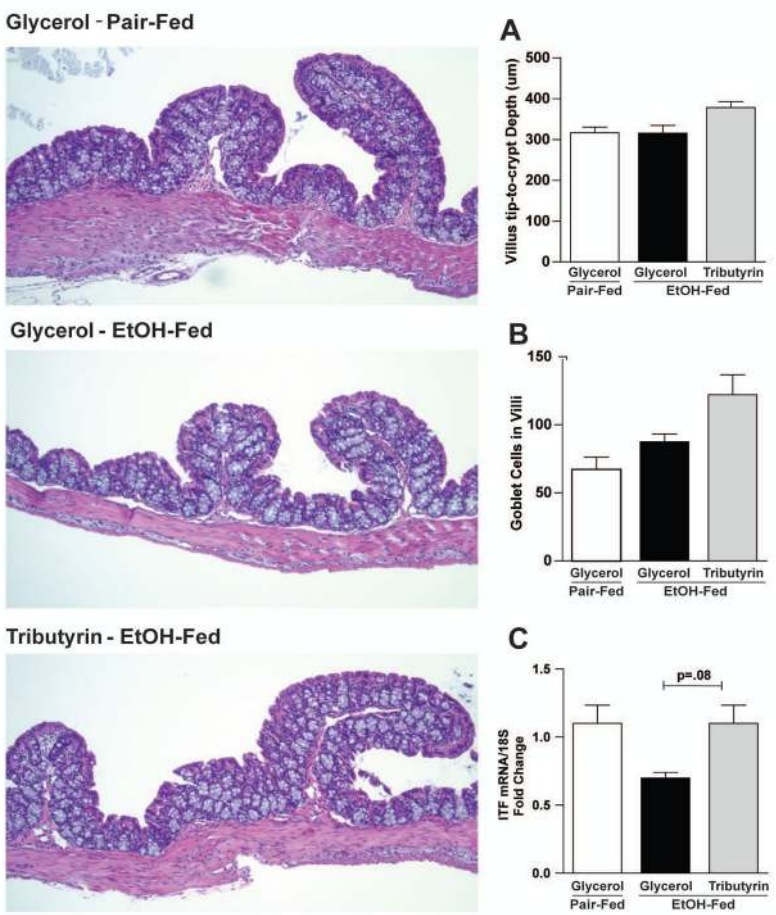

Figure 1. Histopathology of proximal colon in response to ethanol and tributyrin

Mice were fed an EtOH (5% v/v) containing liquid diet or pair-fed a diet with maltose-dextrin isocalorically substituted for ethanol for 10 days. Diets were supplemented with glycerol or tributyrin (5 mM). Mice were then treated with a single 5 g/kg gavage of ethanol the next day containing glycerol or tributyrin (2.5 mM). At 9 hr post-gavage, proximal colon was collected and used to prepare RNA or embedded in OCT for histology. Sections were stained with hematoxylin and eosin and bright-field images captured and analyzed. A) Number of goblet cells/villi were enumerated. B) Villus tip-to-crypt depth was measured (um); 10 crypts per section were evaluated. C) Expression of ITF mRNA was detected in proximal colon using qRT-PCR. D) Representative H&E histological sections of proximal colon from each treatment group are shown. The images are taken by Olympus BX41 microscope with 100× magnification (10×10).

Images are representative of at least replicate images captured per mouse in 4–6 mice per treatment group. Data are the mean ± SEM.

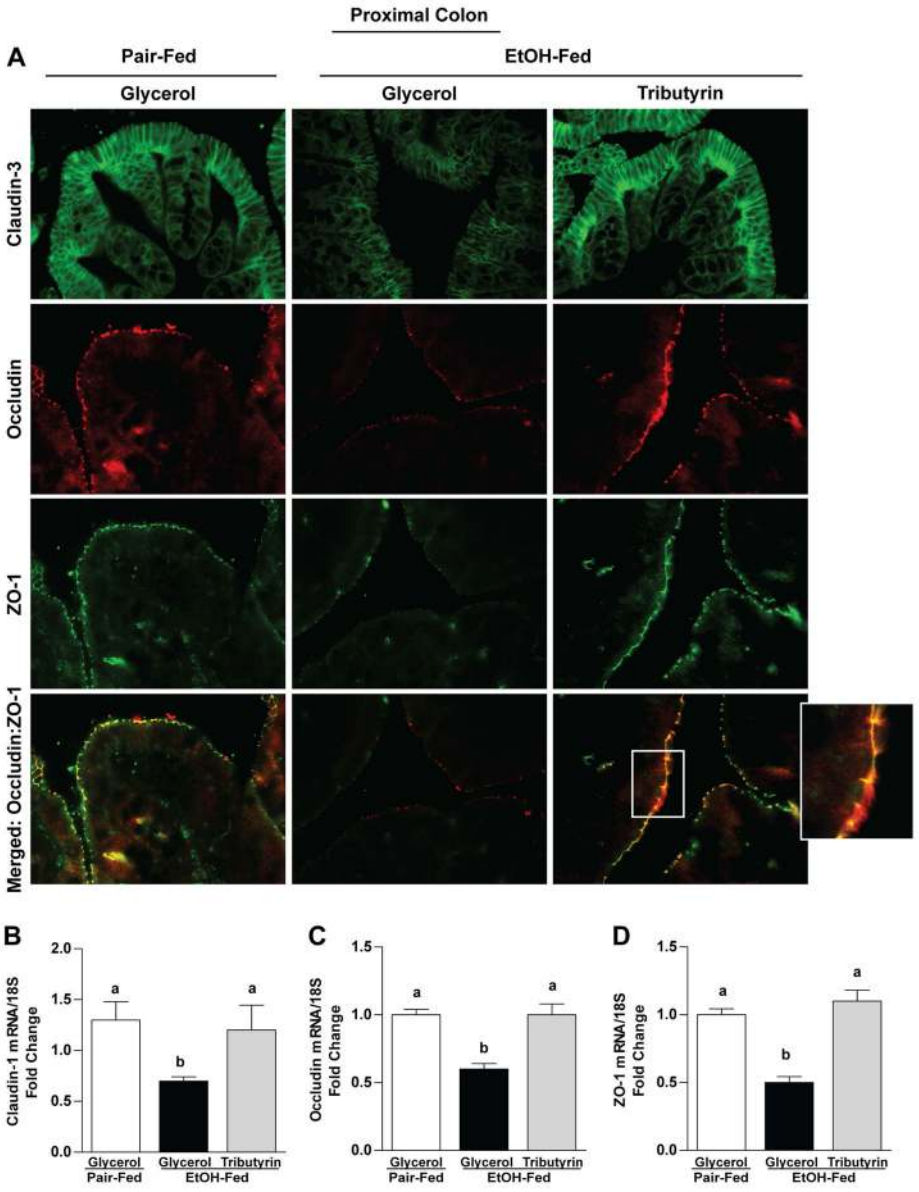

Figure 2. Effects of tributyrin treatment on TJ protein expression in proximal colon

Mice were treated as described in Figure 1. Proximal colon was collected and used to prepare RNA or embedded in OCT for histology. A) Claudin-3 (green), occludin (red) and ZO-1(green) were visualized by immunohistochemistry in sections of proximal colon frozen in OCT. A selected area was cropped and enlarged. All images were acquired using a 40× objective. Images are representative of at least replicate images captured per mouse in 4–6 mice per treatment group. B–D) Expression of claudin-1, occludin, and ZO-1 mRNA was detected in the proximal colon of mice using qRT-PCR. Data are the mean ± SEM. Values with different alphabetical superscripts were significantly different from each other, $p < 0.05$.

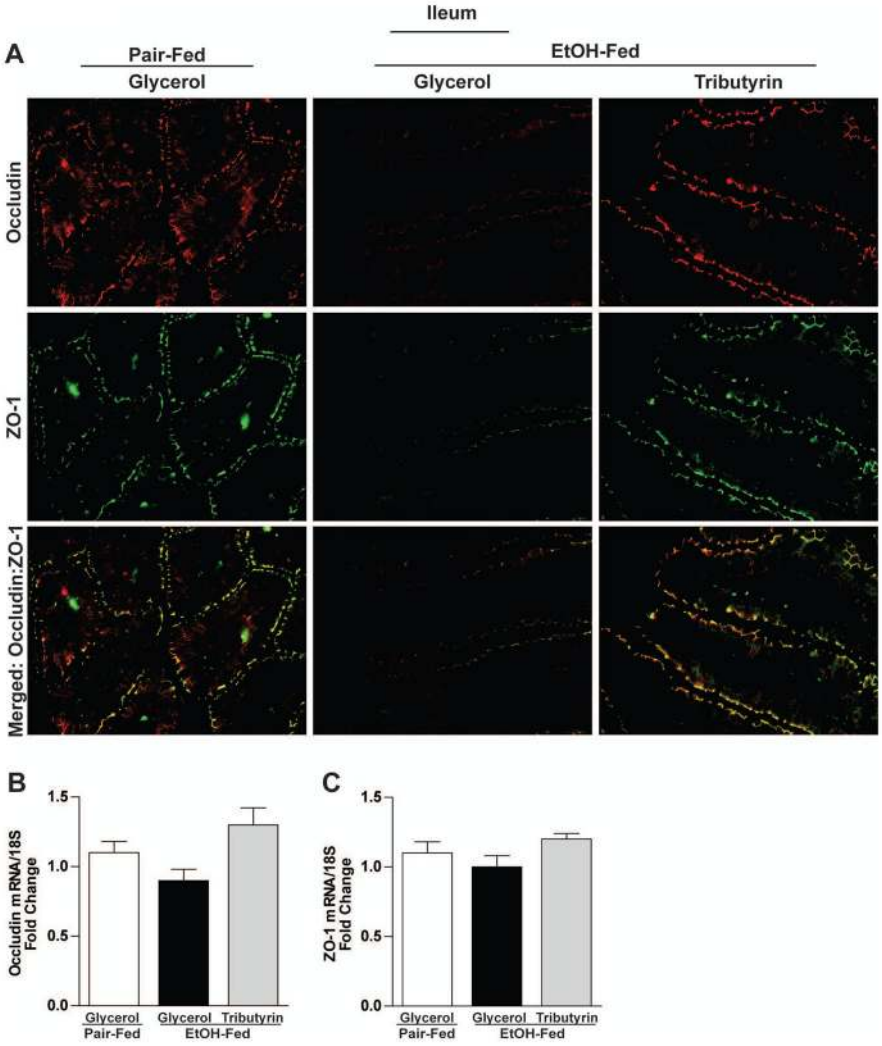

Figure 3. Effects of tributyrin treatment on TJ protein expression in the ileum

Mice were treated as described in Figure 1. Ileum was collected and used to prepare RNA or embedded in OCT for histology. A) Occludin (red) and ZO-1(green) were visualized by immunohistochemistry in sections of ileum frozen in OCT. All images were acquired using a 40× objective. Images are representative of at least replicate images captured per mouse in 4–6 mice per treatment group. B & C) Expression of occludin and ZO-1 mRNA was detected in the ileum of mice using qRT-PCR. Data are the mean ± SEM. Values with different alphabetical superscripts were significantly different from each other, $p < 0.05$.

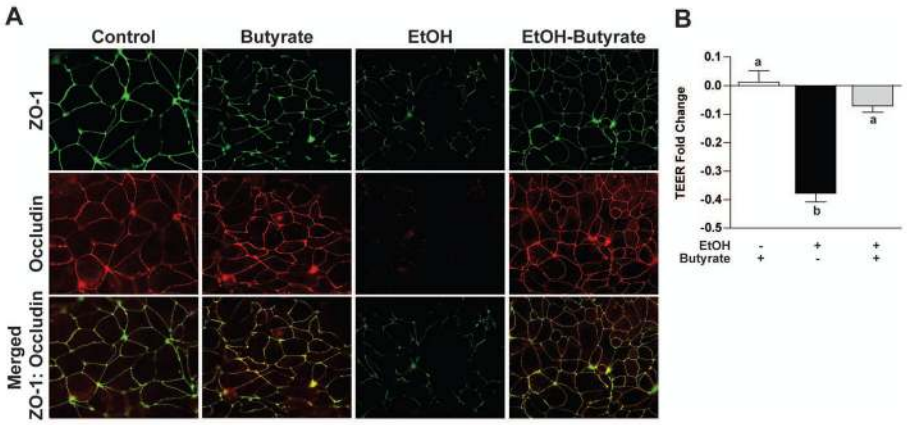

Figure 4. Effect of butyrate on stability of TJ proteins and TEER reduced by EtOH

Human intestinal epithelial cells (Caco2) were grown to confluency on inserts and then pretreated for 18 hrs with sodium butyrate (5 mM). Cells were then challenged with 40 mM ethanol for 3 h and expression of TJ proteins and transepithelial electrical resistance (TEER) was assessed. A) Expression of Occludin (red) and ZO-1(green) was visualized by immunocytochemistry in Caco2 cells fixed in ice-cold methanol. All images were acquired using a 40× objective. Images are representative of at least replicate images captured in three independent experiments. B) A World Precision epithelial volt/ohm meter electrical resistance system was used to measure TEER. TEER values represent relative fold changes compared to cells not challenged with ethanol and/or butyrate. Data are the mean ± SEM of three experiments performed in duplicate. Values with different alphabetical superscripts were significantly different from each other, $p < 0.05$.

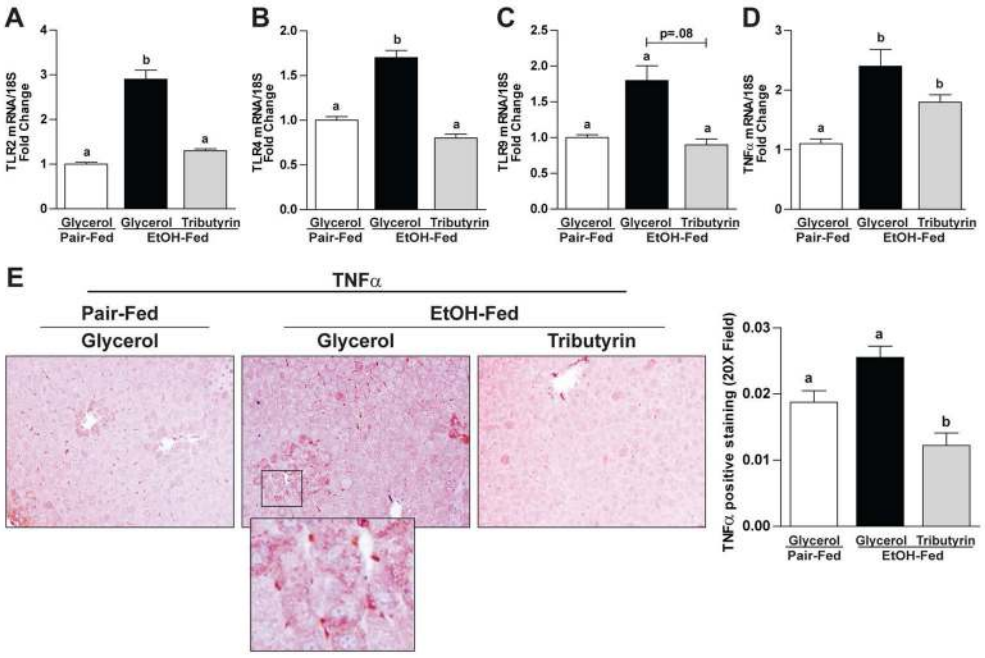

Figure 5. Effects of tributyrin on hepatic expression of TLR and the inflammatory cytokine TNF-α following chronic-binge ethanol exposure

Mice were treated as described in Figure 1. At 9 hours post-gavage, liver was excised and used to prepare RNA or embedded in formalin for IHC. A–D) Expression of TLR2, TLR4 and TLR9 and TNFα mRNA was detected in mouse livers using qRT-PCR. E) TNFα protein was evaluated by immunohistochemistry in paraffin embedded liver tissue. All images were acquired using a 40× objective. TNF-α positive areas were quantified using Image-Pro Plus software and analyzed. Values represent means ±SEM. n = 4–6 mice per treatment group. Values with different alphabetical superscripts were significantly different from each other, $p < 0.05$.

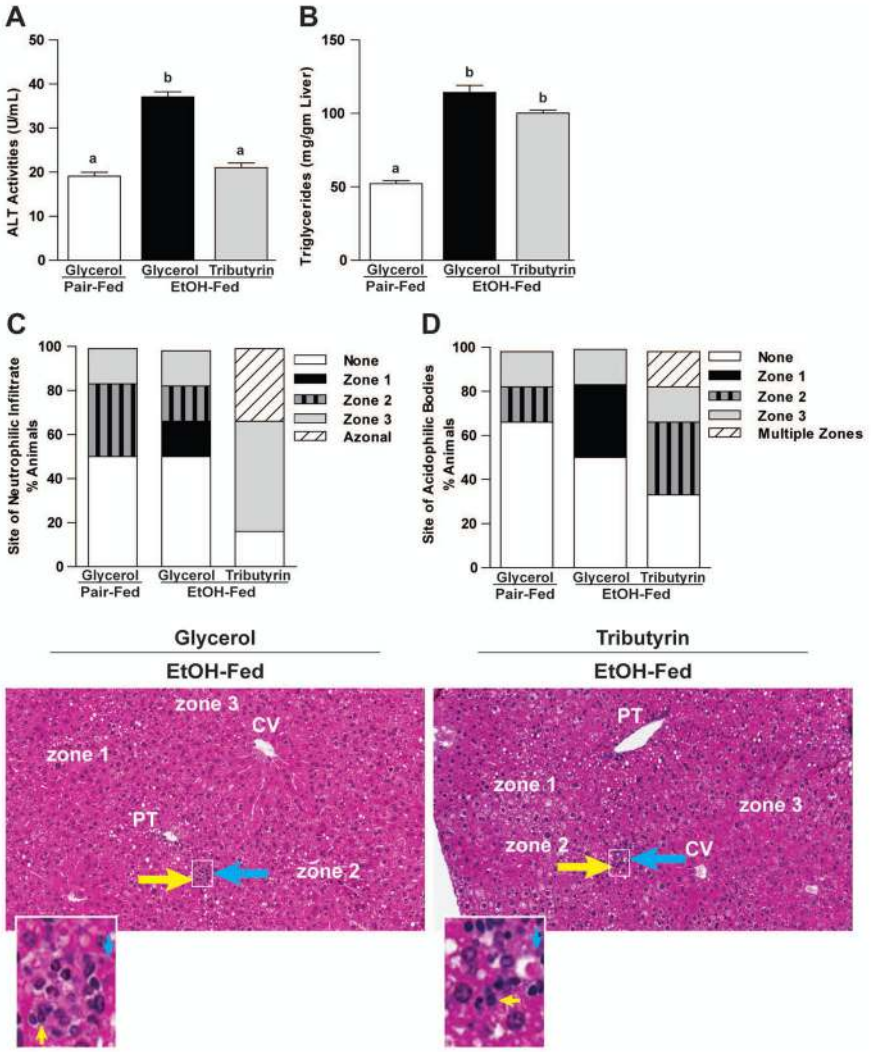

Figure 6. Effects of tributyrin on hepatic injury and zonation of neutrophilic infiltrate and acidophilic bodies following chronic-binge ethanol exposure

Mice were treated as described in Figure 1. Mice were euthanized 9-hours post-ethanol gavage. A & B) Plasma was separated from blood collected from the posterior vena cava. Activity of ALT was measured in plasma. Hepatic triglyceride content was measured in whole liver homogenates. C–E) Liver was excised, fixed in formalin, embedded in paraffin and later stained with hematoxylin and eosin for histologic analysis. Quantitative assessment of the neutrophilic infiltrate and acidophilic bodies are shown. Bars represent percentage of mice in each group exhibiting the designated number of foci of neutrophilic infiltrates per high power field, acidophilic bodies and their zonal distribution in the liver (zone 1, 2 or 3; azonal: no recognizable pattern; multiple zones, multifocal but possible throughout the tissue with inconsistent distribution). Representative H&E histological sections of livers are shown for the study groups. Yellow arrows indicate neutrophilic infiltrates; blue arrows indicate acidophil bodies. (H&E stain, 100×).

Table 1

Primer sequences for real-time RT-PCR

Gene	Sequences (Forward/Reverse 5′-3′)	
ITF	TGGGATAGCTGCAGATTACG	GCCACAGTCCACTCTGACAT
Claudin-1	CGGGCAGATACAGTGCAAAG	ACTTCATGCCAATGGTGGAC
ZO-1	TGGGAACAGCACACAGTGAC	GCTGGCCCTCCTTTTAACAC
Occludin	ACCCGAAGAAAGATGGATCG	CATAGTCAGATGGGGGTGGA
TNFα	CCCTCACACTCAGATCATCTTCT	GCTACGACGTGGGCTACAG
TLR2	TGCTTTCCTGCTGGAGATTT	TGTAACGCAACAGCTTCAGG
TLR4	ATGGCATGGCTTACACCACC	GAGGCCAATTTTGTCTCCACA
TLR9	TCAGCCACAACATTCTCAAGAC	GAGGGTTGCTTCTCACGTCTA
18S	ACGGAAGGGCACCACCAGGA	CACCACCACCCACGGAATCG